NPS ARCHIVE
1997.09
MACMANNIS, A.

NAVAL POSTGRADUATE SCHOOL
Monterey, California

THESIS

THE DESIGN OF THE NAVAL POSTGRADUATE SCHOOL'S ULTRAVIOLET IMAGING SPECTROMETER (NUVIS)

by

Andrew R. MacMannis

September 1997

Thesis Advisor: David D. Cleary

Thesis
M2524

Approved for public release; distribution is unlimited.

DUDLEY KNOX LIBRARY
NAVAL POSTGRADUATE SCHOOL
MONTEREY CA 93943-5101

DUDLEY KNOX LIBRARY
NAVAL POSTGRADUATE SCHOOL
MONTEREY CA 93943-5101

REPORT DOCUMENTATION PAGE

Form Approved
OMB No. 0704-0188

Public reporting burden for this collection of information is estimated to average 1 hour per response, including the time for reviewing instruction, searching existing data sources, gathering and maintaining the data needed, and completing and reviewing the collection of information. Send comments regarding this burden estimate or any other aspect of this collection of information, including suggestions for reducing this burden, to Washington headquarters Services, Directorate for Information Operations and Reports, 1215 Jefferson Davis Highway, Suite 1204, Arlington, VA 22202-4302, and to the Office of Management and Budget, Paperwork Reduction Project (0704-0188) Washington DC 20503.

AGENCY USE ONLY *(Leave blank)*	2. REPORT DATE	3. REPORT TYPE AND DATES COVERED
	September 1997	Master's Thesis

4. TITLE AND SUBTITLE
THE DESIGN OF THE NAVAL POSTGRADUATE SCHOOL'S ULTRAVIOLET IMAGING SPECTROMETER (NUVIS)

5. FUNDING NUMBERS

6. AUTHOR(S)
Andrew R. MacMannis

7 PERFORMING ORGANIZATION NAME(S) AND ADDRESS(ES)
Naval Postgraduate School
Monterey CA 93943-5000

8. PERFORMING ORGANIZATION REPORT NUMBER:

9. SPONSORING/MONITORING AGENCY NAME(S) AND ADDRESS(ES)

10. SPONSORING/MONITORING AGENCY REPORT NUMBER:

11 SUPPLEMENTARY NOTES
The views expressed in this thesis are those of the author and do not reflect the official policy or position of the Department of Defense or the US Government.

12a DISTRIBUTION/AVAILABILITY STATEMENT
Approved for public release; distribution is unlimited.

12b. DISTRIBUTION CODE

13 ABSTRACT *(maximum 200 words)*

Hyperspectral imaging spectrometers are remote sensing instuments capable of producing an image cube comprised of a two-dimensional scene and the corresponding spectra of each scene element. Remote sensing is growing in civilian applications and support of military operations. Civilian applications vary from plant species identification, stress measurement, leaf water content and canopy chemistry to geological identification and mapping. Military applications include target identification and classification, bomb damage assessment, terrain or area utilization and rocket plume identification.

This thesis describes the fabrication and alignment of the NPS Ultraviolet Imaging Spectrometer (NUVIS). NUVIS is a hyperspectral imaging spectrometer designed to investigate the added value of the ultraviolet region of the spectrum. The spectrometer is comprised of a telescope assembly using an off-axis parabolic mirror, a slit, a flat-field imaging diffraction grating and a camera assembly. This is the first part of a continuing project to build, test and use this sensor for support of military operations.

14 SUBJECT TERMS	15 NUMBER OF PAGES.
Hyperspectral Imaging, Ultraviolet, Remote Sensing, Support to Military Operations	65
	16 PRICE CODE

17 SECURITY CLASSIFICATION OF REPORT	18. SECURITY CLASSIFICATION OF THIS PAGE	19. SECURITY CLASSIFICATION OF ABSTRACT	20 LIMITATION OF ABSTRACT
Unclassified	Unclassified	Unclassified	UL

NSN 7540-01-280-5500

Standard Form 298 (Rev. 2-89)

Prescribed by ANSI Std 239-18

Approved for public release; distribution is unlimited.

THE DESIGN OF THE NAVAL POSTGRADUATE SCHOOL'S ULTRAVIOLET IMAGING SPECTROMETER

Andrew R. MacMannis
Major, United States Marine Corps
B.S., The Pennsylvania State University, 1984

Submitted in partial fulfillment of the
requirements for the degree of

MASTER OF SCIENCE IN APPLIED PHYSICS

from the

NAVAL POSTGRADUATE SCHOOL
September 1997

NPS Archive
1997.09
MacMannis, A.

T Ass.i
M2624
c.2

DUDLEY KNOX LIBRARY
NAVAL POSTGRADUATE SCHOOL
MONTEREY CA 93943-5101

ABSTRACT

Hyperspectral imaging spectrometers are remote sensing instruments capable of producing an image cube comprised of a two-dimensional scene and the corresponding spectra of each scene element. Remote sensing is growing in civilian applications and support of military operations. Civilian applications vary from plant species identification, stress mearsurement, leaf water content and canopy chemistry to geological identification and mapping. Military applications include target identification and classification, bomb damage assessment, terrain or area utilization and rocket plume identification.

This thesis describes the fabrication and alignment of the NPS Ultraviolet Imaging Spectrometer (NUVIS). NUVIS is a hyperspectral imaging spectrometer designed to investigate the added value of the ultraviolet region of the spectrum. The spectrometer is comprised of a telescope assembly using an off-axis parabolic mirror, a slit, a flat-field imaging diffraction grating and a camera assembly. This is the first part of a continuing project to build, test and use this sensor for support of military operations.

TABLE OF CONTENTS

I. INTRODUCTION 1

II. ELECTROMAGNETIC SPECTRUM 5
A. ELECTROMAGNETIC RADIATION 5
B. LIGHT INTERACTIONS WITH THE ATMOSPHERE 7
1. Scattering 7
2. Refraction 8
3. Absorption 9
C. LIGHT INTERACTIONS WITH SURFACES 10
1. Reflection 10
2. Transmission 11
3. Absorption 11
D. SPECTRAL SIGNATURES 12

III. IMAGING SPECTROMETERS 15
A. AN IMAGE 15
B. SPECTRAL RESOLUTION AND REMOTE SENSING CLASSIFICATION 16
1. Multispectral Sensors 17
2. Hyperspectral Sensors 18
3. Ultraspectral Sensors 19

IV. NAVAL POSTGRADUATE SCHOOL'S ULTRAVIOLET IMAGING SPECTROMETER (NUVIS) 21
A. TELESCOPE ASSEMBLY 22
1. Filter Window 23
2. Scanning Mirror Assembly 24
3. Telescope Housing 25
4. Telescope Mirror 25
B. ENTRANCE SLIT 25
C. REFLECTION GRATING 28
D. CAMERA ASSEMBLY 30
1. Image Intensifier 31
a. Filter Window 32
b. S-20 Photocathode 32
c. Microchannel Plate Assembly 35
d. P-20AF Phosphor Screen 37
2. Charge Coupled Device 38

V. ALIGNMENT, PLACEMENT AND CONSTRUCTION 43
A. TELESCOPE MIRROR ALIGNMENT AND ENTRANCE SLIT PLACEMENT 43

B. REFLECTION GRATING AND CAMERA ASSEMBLY PLACEMENT 45
C. ENTRANCE SLIT CONSTRUCTION 45

VI. SUMMARY AND RECOMMENDATIONS 47

LIST OF REFERENCES 49

INITIAL DISTRIBUTION LIST 51

LIST OF FIGURES

Figure 1: The Electromagnetic Spectrum. From Kuo-Nan Liou (1980). 6
Figure 2: Spectral irradiance distribution curves related to the sun; (1) observed solar irradiance at the top of the atmosphere, (2) observed solar irradiance at sea level. The shaded area represents absorption in a clear atmosphere. From Kuo-Nan Liou (1980) 7
Figure 3: Spectral signatures. From Collins (1996). 13
Figure 4: Comparison of Reflectance of four spectral signatures at two different wavelengths. From Collins (1996). 14
Figure 5: An image cube. From Johnson (1996) 16
Figure 6: Classification of spectral imaging. From Multispectral Users Guide (1995).. 17
Figure 7: The Naval Postgraduate School's Ultraviolet Imaging Spectromete (NUVIS). 22
Figure 8: The entrance slit holder. 27
Figure 9: the entrance slit before razor blades are attached. 27
Figure 10: Diffraction geometry. From Milton Ray Company (1994). 28
Figure 11: Geometry of the entrance slit and the detector relative to the grating recommended by Instruments S.A., Inc. After Jiang (1997). 30
Figure 12: The sensitivity of the Pulnix TM-745 high resolution camera. From Pulnix.32
Figure 13: Photocathode sensitivity and quantum efficiency. From DeBarry (1997). ... 33
Figure 14: Photoelectric effect in a semiconductor. After Reike (1994). 34
Figure 15: MCP construction. From Hamamatsu Photonics (1985). 35
Figure 16: Electric representation of electron amplification. From Hamamatsu Photonics. 36
Figure 17: Process of luminescence of a phosphor. From Reike (1994). 38
Figure 18: Charge collection at a single pixel of a CCD: (a) illustrates the collection of free charge carriers at the S1O2 interface, (b) shows formation of a potential well after a voltage is applied, (c) shows collection of charge carriers in the potential well. From Reike (1994) 40
Figure 19: The alignment tool used to place razor blade on entrance slit 46

LIST OF TABLES

Table 1. Landsat Thematic Mapper Spectral Bands. From Collins. (1996)..... 18
Table 2. Spectral Band Characteristics of several Hyperspectral Sensors.
From Collins (1996). 19

I. INTRODUCTION

A thesis is a long road with many turns. My journey began with an interest in imagery intelligence. This interest stems from a fascination with products seen as an infantry officer in the Fleet Marine Force. Where these pictures come from and how they are produced has always been a mystery until recently. This thesis was my opportunity to learn more in this area. Upon investigation, I found a large and growing DOD interest in these same areas.

Such growth has produced the Hyperspectral MASINT Support for Military Operations (HYMSMO) program office in May, 1994. MASINT stands for Measurement and Signals Intelligence. This program office initiated by the Central MASINT Office (CMO) has grown exponentially ever since. Objectives of the program office include:

1. Explore and evaluate the potential utility of hyperspectral collection and exploitation techniques in satisfying the time sensitive information needs of military operations and/or critical intelligence applications.
2. Demonstrate the power of nonliteral exploitation techniques.
3. Develop practical and inexpensive OpMASINT system concepts.
4. Transfer technology and "lessons learned" to the system acquisition program offices and potential users of the Defense and Intelligence Communities.
5. Advocate the operational role and value of Spectroradiometric MASINT.

This shows the wide variety and growing interest in spectral imagery.

Advances in remote sensing include developing sensors and the software to spot, locate and identify military items of interest. For example, there will come a time soon when a picture is processed real time that identifies objects of military value within the

scene. Military value may consist of identification or classification of vehicles and camouflage, bomb damage assessment, and almost any other physical detail one could ask for regardless of terrain, vegetation or weather. This scenario is not far off and hyperspectral imaging is one sensor technique making progress in this area.

A hyperspectral imaging device measures reflected and emitted electromagnetic radiation from everything in a scene. From this data, software programs can identify or pick out specifics relative to a library of known knowledge. Identification is possible from as far away as hundreds of kilometers or as close as meters. The size of identifiable material is dependent on many parameters but today it is possible to identify objects within one square meter. Also these remote sensors are capable of integrating location with spectral identification. Identification discrimination techniques are being discovered every day and many people are working on improving the quality of the product. One organization conducting this research is The Naval Postgraduate School.

A hyperspectral imaging device is located at the Naval Postgraduate School. The NPS Ultraviolet Imaging Spectrometer (NUVIS) has evolved over several years. Johnson (1996) attempted to modify an existing spectrometer to one that was capable of imaging. Johnson's DUUVIS (Dual Use Ultraviolet Imaging Spectrometer) was originally built with a tracking mirror, a telescope, and a Ebert-Fastie design spectrometer. Because of the desire to investigate the ultraviolet region and the small amounts of ultraviolet light in the atmosphere, an image intensifier was put on the end of a CCD camera for the collection of data. My thesis began as a desire to design an experiment to make ultraviolet observations of targets, collect the data and analyze the data to quantify the abilities of DUUVIS.

Unfortunately, upon investigation into the abilities of DUUVIS before taking measurements, we found that the image quality of the device was inadequate for data analysis. The point spread function or spot size on the camera, one of the quality determining factors, was found to be very large. Spot size needs to be small. This anomaly was verified using a ray tracing program designed at the Naval Postgraduate School by Atkinson (1993). A decision was needed to either modify DUUVIS again or build another device.

After considering the possible modifications of DUUVIS, it was determined that we would have to replace almost every optical element, and resize the instrument for a new housing assembly while only achieving moderately better results. Thus the decision was made to build anew. Work began on the design of a hyperspectral imaging spectrometer which produces quality images and can be easily modified to observe not only portions of the UV spectrum, but other spectral ranges as well. This new instrument was then renamed the Naval Postgraduate School's Ultraviolet Imaging Spectrometer (NUVIS).

My thesis work involves the building of this new hyperspectral imaging device in collaboration with another student, Hooks (1997). My responsibilities were primarily associated with the design blueprint and the optics. This includes the focusing mirror, the slit, and the reflectance grating. Hooks was responsible for the scanning mirror with associated motor controls, the camera and the computer with associated software. This thesis will cover more depth associated with the parts for which I was responsible. Before getting into the actual design, we must first provide background for the

inexperienced remote sensing reader. This information is very basic and is where I started when beginning my research into this area.

II. ELECTROMAGNETIC SPECTRUM

A. ELECTROMAGNETIC RADIATION

Spectroscopy, the physics that deals with the interpretation of electromagnetic radiation begins with some depth of discussion on light and its characteristics as it enters the atmosphere and interacts with physical materials. Light, emitted from the sun, consists of electromagnetic energy and is explained in two very different manners. First, light can be explained as photons. You can think of photons as particles or discreet bundles of energy that travel from point to point. The second explanation of light is as a propagating electromagnetic wave that varies in magnitude and direction. Amplitude and frequency (or wavelength) characterizes these waves. Both explanations of light will be used throughout this paper. All light has associated energy that is proportional to its frequency.

Electromagnetic energy is produced by changes in energy levels of electrons, acceleration of electrical charges, decay of radioactive substances, or the thermal motion of atoms and molecules. Detectors or sensors record this energy for use in analysis. Passive light detectors record the reflected energy originally produced by the sun or the thermal energy emmited by the target. Active instruments generate electromagnetic energy and record the return signal. The electromagnetic energy recorded consists of waves with different wavelengths. These waves produce a spectrum which physicists have arbitrarily segmented into major divisions of wavelength as described in Figure 1. The spectrum recorded by a sensor is affected by many interactions between the sun and the sensor. We must therefore talk about those interactions before we talk about the detectors.

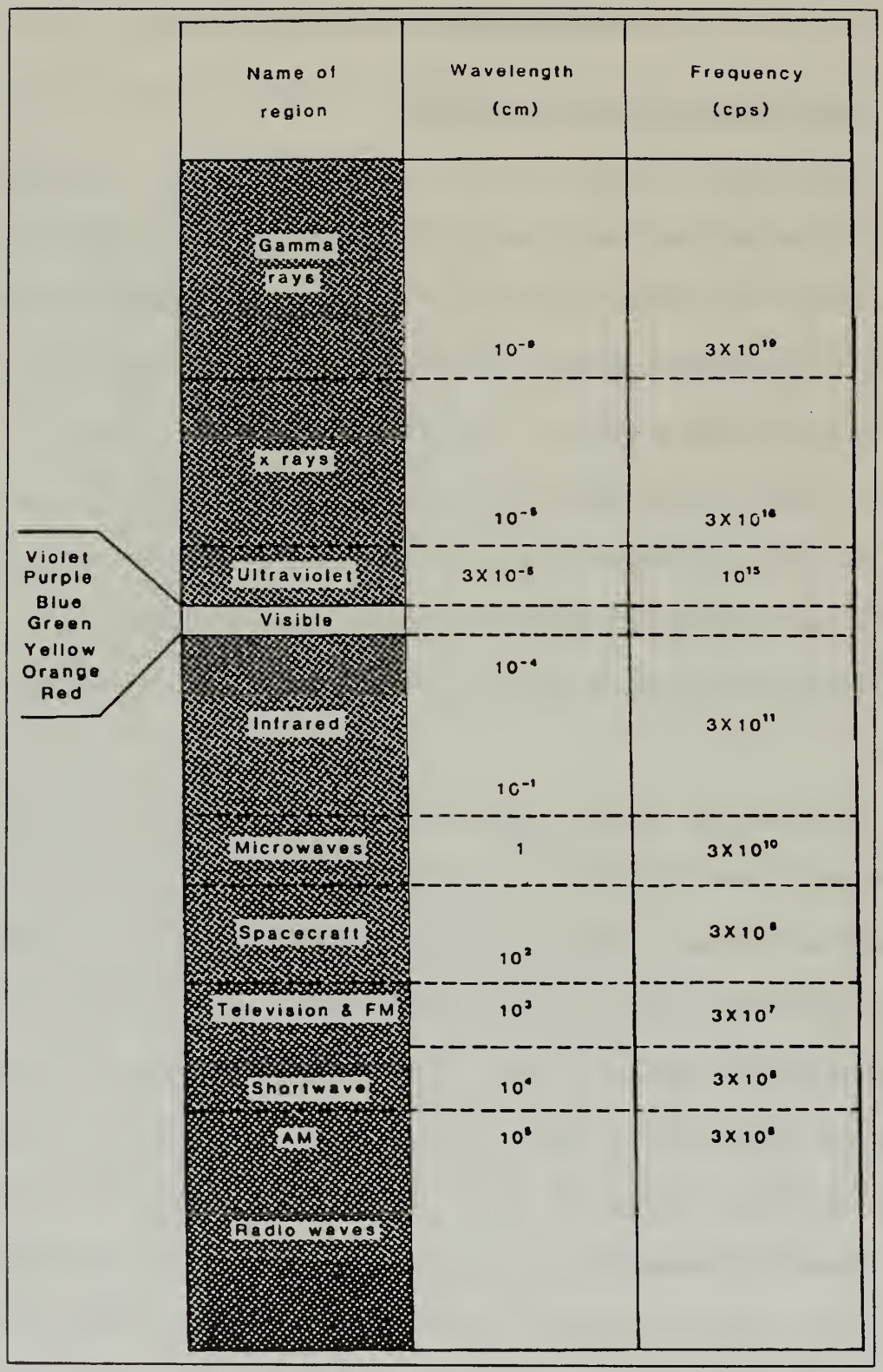


Figure 1: The Electromagnetic Spectrum. From Kuo-Nan Liou (1980).

B. LIGHT INTERACTIONS WITH THE ATMOSPHERE

The solar spectrum changes very little between the sun and earth. It isn't until the radiation reaches the Earth's atmosphere that the solar spectrum changes appreciably. Interactions within the atmosphere will alter the solar spectrum measured by a detector. Figure 2 shows the solar irradiance as a function of wavelength at both the top of the atmosphere and at the earth's surface. Scattering, refraction (bending) and absorption are interactions that reduce the transmittance of light within the atmosphere.

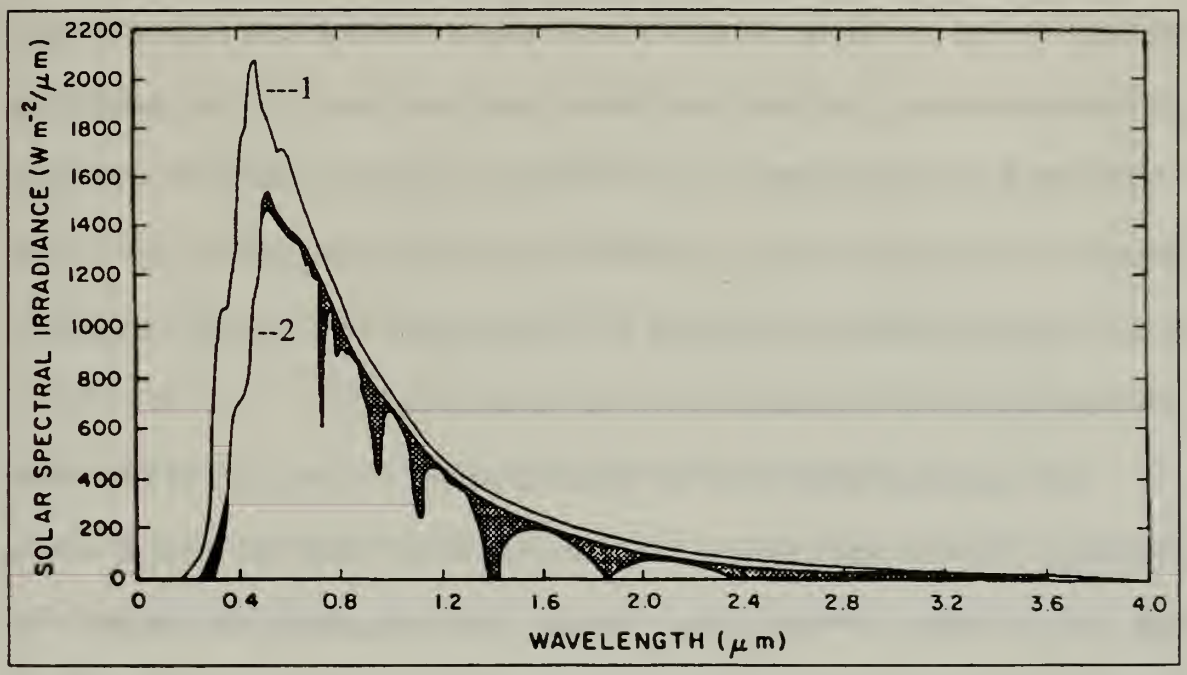


Figure 2: Spectral irradiance distribution curves related to the sun; (1) observed solar irradiance at the top of the atmosphere, (2) observed solar irradiance at sea level. The shaded area represents absorption in a clear atmosphere. From Kuo-Nan Liou (1980).

1. Scattering

Scattering is the redirection of the waves by particles or molecules suspended within the atmosphere. The scattered photons can be redirected in any direction. The effects of scattering are numerous. Scattering produces the blue sky during the day. It

allows us to see in the shadows out of direct sunlight. Scattering tends to make dark images lighter and light images darker. With respect to image sensing, scattering forces detectors to record background brightness associated with a scene as well as recording light from a target (reduces contrast). Scattering deflects some light from a target away from the sensor decreasing spatial detail (fuzzy images).

There are three basic scattering mechanisms: Rayleigh, Mie, and Non-selective. The reletive importance of each depends on the size of the particle and the wavelength of the light. Rayleigh scattering, sometimes called clear atmosphere scattering, takes place predominately in the upper atmosphere due to atmospheric gasses. These atmospheric particles have diameters smaller than the wavelength of the light. Relative to Mie and non-selective scattering, the cross section for Rayleigh scattering increases as $1/\lambda^4$. This is the dominant scattering mechanism in the ultraviolet. This effect is mostly at elevations around 9 to 10 kilometers above the surface of the earth.

MIE scattering occurs when the scattering particle is comparible in size to the wavelength. Particles which produce MIE scattering in the visible and infrared include dust, pollen, smoke and water drops. Effects of MIE scattering are dependent on wavelength and affect electromagnetic radiation mostly in the visible spectral region.

Non-selective scattering is caused by particles with a much larger diameter than the incident wavelength. This type of scattering is not wavelength dependent and is the primary cause of haze.

2. Refraction

Refraction is the bending of light as it passes through any medium with a gradient in optical density. This density change can be discreet as with an air-glass interface, or it

can be continuous as in the atmosphere. Diffraction causes mirages on a hot day and can severely degrade spectral signatures taken over a large distance. The larger the change in density the larger the refraction.

3. Absorption

Absorption is broken into two types: general and selective. General absorption reduces the intensity of light at all wavelengths nearly the same. No material has been found to absorb all wavelengths exactly the same, but there are some materials that can be approximated as absorbing equally over a wide range of wavelengths. Selective absorption is dependent on wavelength. Colored surfaces owe their color to selective absorption. As an example green grass will absorb the wavelengths which correspond to red and blue. What is not absorbed but is reflected in the visible region will produce the green color. These wavelengths are scattered with enough intensity to reach your eye and record the green color. Absorption can take place while light is traveling through solids, liquids or gasses. In the atmosphere mostly gasses affect absorption.

Most absorption in the ultraviolet and visible regions takes place due to diatomic and tri-atomic molecular electronic, vibrational and rotational transitions from one quantum state to another. In the ultraviolet region of the spectrum, oxygen and nitrogen species dominate absorption. O_2, O_3, N_2, CO_2, H_2O, O and N are all examples of ultraviolet absorbers. The middle atmosphere has a large ozone (O_3) layer at approximately 30 km. Most of the ultraviolet absorption in this region is due to the ozone. Other absorption is small compared to O_3 absorption and is less important when taking measurements at altitudes under 80-km.

The scattering, refraction and absorption interactions within the atmosphere are important and need to be reckoned with while analyzing any data received by a detector. These interactions are not the only consequences of light traveling through the atmosphere into a detector. For us to be able to use the spectrum of light it must first interact with surfaces within a target area.

C. LIGHT INTERACTIONS WITH SURFACES

After light passes through the atmosphere or even while passing through, it will interact with surfaces such as aircraft, buildings, vegetation or soil. These interactions are affected by the irregularities of the surfaces, the wavelength of light and the angle of incidence. Interactions with surfaces are divided into three areas: reflection, transmission and absorption.

1. Reflection

Reflection can be characterized by the return of light waves from a surface. The term reflectance is a ratio of an amount of light returned from a surface to the total amount of light that initially hits the surface. The light that was not reflected has been transmitted through the surface or absorbed by the surface. The type of reflection is determined by the size of the surface irregularities relative to the incident wavelength of light. There are two basic types of reflection: specular and diffuse.

Specular reflection, sometimes called mirror reflection, is light returned from a smooth surface. A smooth surface is defined as having irregular deformations in the surface which are smaller than the wavelength of incident light. Light will be reflected in one direction with the reflected angle equal in magnitude to the angle of incidence. This type of reflectance affects remote sensing depending on where the target is relative to the

incident light and sensor. If the sensor is not at the precise angle relative to the sun and the target, detection of the specularly reflected signal will not occur. Fortunately most surfaces are not solely specular reflectors.

Diffuse reflection can be thought of as reflection from a rough surface relative to the the wavelength of incident light. A rough surface has irregularities comparable to or larger than the incident wavelengths of light. It is also called isotropic or Lambertian reflectance. The incident light is scattered in all directions. Most surfaces are diffuse to some extent. A perfectly diffuse surface is termed a Lambertian surface and reflects light with a cosine dependence. When encountering surfaces within a target area, there is a mix of diffuse and specular properties.

2. Transmission

Transmission is light traveling through a surface and is wavelength dependent. Transmission is the ratio of the amount of transmitted light relative to the amount of incident light. Some objects that do not transmit light in the visible can transmit light at other wavelengths. This ability is one example that explains the usefulness of remote sensing. As an example, some plants that do not transmit visible wavelengths of light can transmit infrared wavelengths. Some infrared sensors can therefor record a spectral return from materials beneath plants. In the ultraviolet region not much research on ultraviolet remote sensing value has been conducted.

3. Absorption

Absorption, whether by interacting with surfaces or interacting within the atmosphere, is the same as described in the previous section. All solids have absorptive qualities dependent on wavelength. A large concern for remote sensing is the absorptive

qualities of the optics and materials used in the sensors. Specifically, the design of an instrument using ultraviolet light must consider of the optical materials used, as most optical materials will absorb ultraviolet light. The amount of absorption, transmission and reflectance of light relative to a target area or scene makes up a spectral signature that can be captured by remote sensors.

D. SPECTRAL SIGNATURES

Everything in nature has a spectral signature. That is to say every thing, natural or man-made will have specific absorption, transmission and reflection qualities. Theoretically, each specific material signature can be identified and catalogued. The value of remote sensing is directly related to the ability to discriminate individual materials within a target area. With today's technology, the ability to catalogue and discriminate is improving. There are still obstacles to discrimination of spectral signatures within a target area. Spectral signatures can change over time. Weather will affect the individual signature you receive. These obstacles will affect your results when comparing them to a library of catalogued signatures. Figure 3 shows some spectral signatures of plants within .4-μm to 1.2-μm. This signature will change on a rainy day and will show a different signature for different times of a year. There are many other factors that effect a spectral signature.

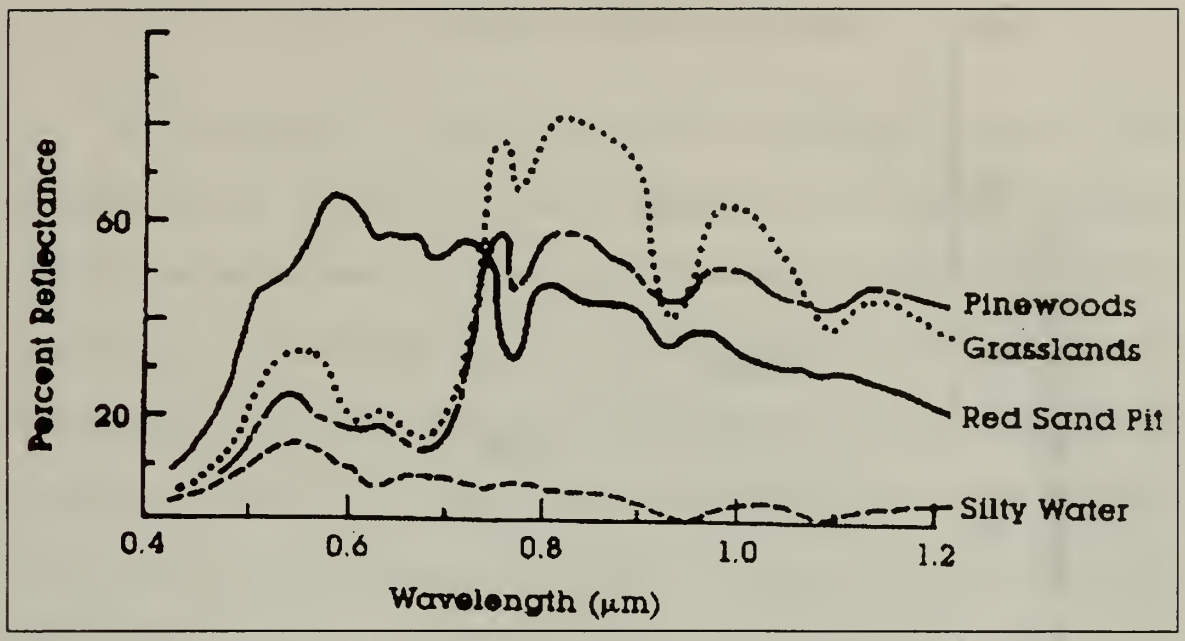


Figure 3: Spectral signatures. From Collins (1996).

In principle factors affecting catalogued spectra can be predicted or measured. Understanding those conditions can improve identification provided there is an accurate, proven method for cataloging. Techniques for cataloging spectra are getting better as are techniques for identifying materials under a host of conditions. One example of a discrimination technique is the comparison of different spectra at different wavelengths as in Figure 4. These plots increase the separability of contrasting materials. This and other techniques are the basis for spectral remote sensing analysis.

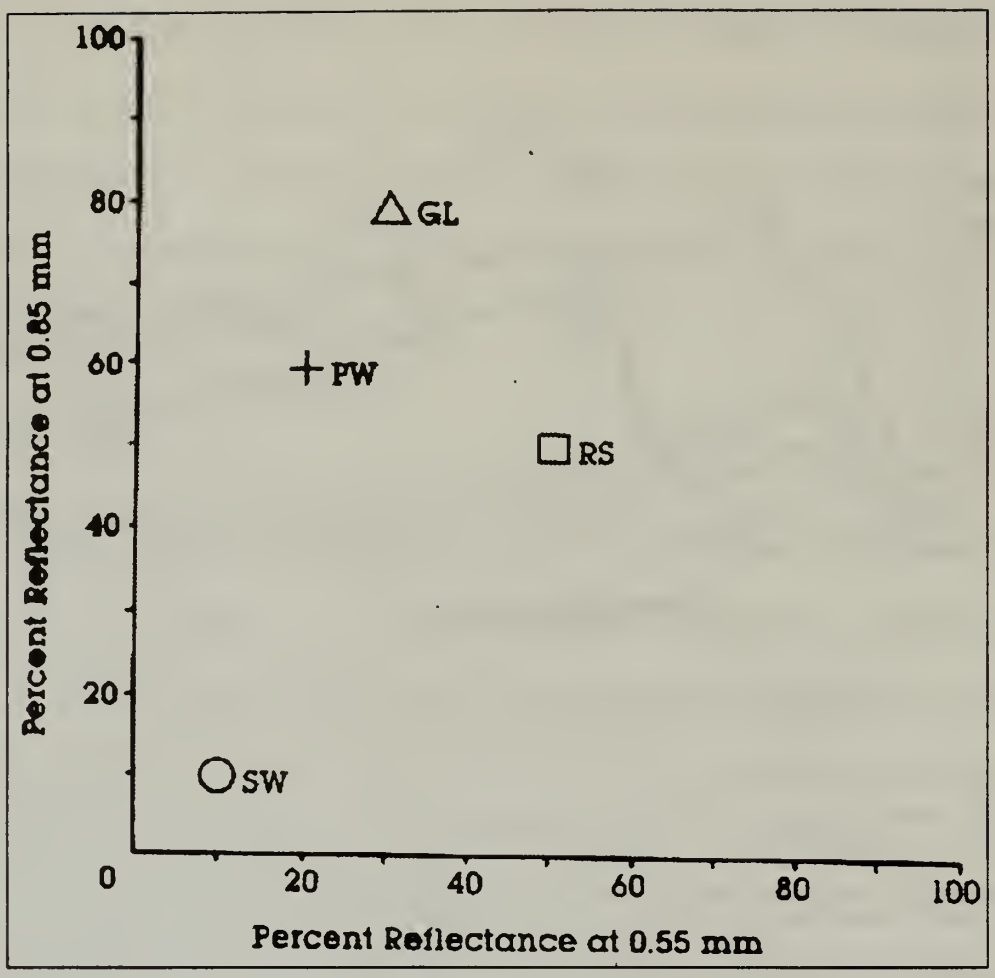


Figure 4: Comparison of Reflectance of four spectral signatures at two different wavelengths. From Collins (1996).

III. IMAGING SPECTROMETERS

The development of imaging spectrometers for remote sensing has seen exponential growth. Although spectrometers to analyze spectra of materials have been around for several hundred years, imaging spectrometers are relatively new. Imaging spectrometers record information on a two-dimensional spatial scene or target area with the associated spectrum. This makes a three-dimensional cube. This technique allows for the analysis of spectra across any given scene. In this chapter we will focus on the nature of an image, spectral definitions as they apply to the image, and the devices used to record spectral imagery.

A. AN IMAGE

In remote sensing, an image is not the same as a photographic image. A remote sensing image is a rendition of features that have spatial and spectral properties. Spatial properties refer to the width or length of an image as in a picture. The spectral properties of an image are the intensities of spectral wavelengths across a scene. A remote sensing image is two dimensional with one dimension spectral and the other dimension spatial. This image is also called a slice. Each image is divided up into many pixels. Each pixel is a square of very small size consisting of a spatial dimension with a small spectral bandwidth. The bandwidth of the pixel is a fraction of the image's bandwidth depending on the number of pixels.

A row of images represents a scan line and is sometimes referred to as a swath. This row of slices adds another spatial dimension completing an image cube, as in Figure 5. Notice one spectral dimension and two spatial dimensions. All image cubes are composed of a three dimensional matrix of pixels. There are several hundred pixels

in each dimension. The number of pixels used and the quality of optics of a sensor determines an image's spectral characteristic.

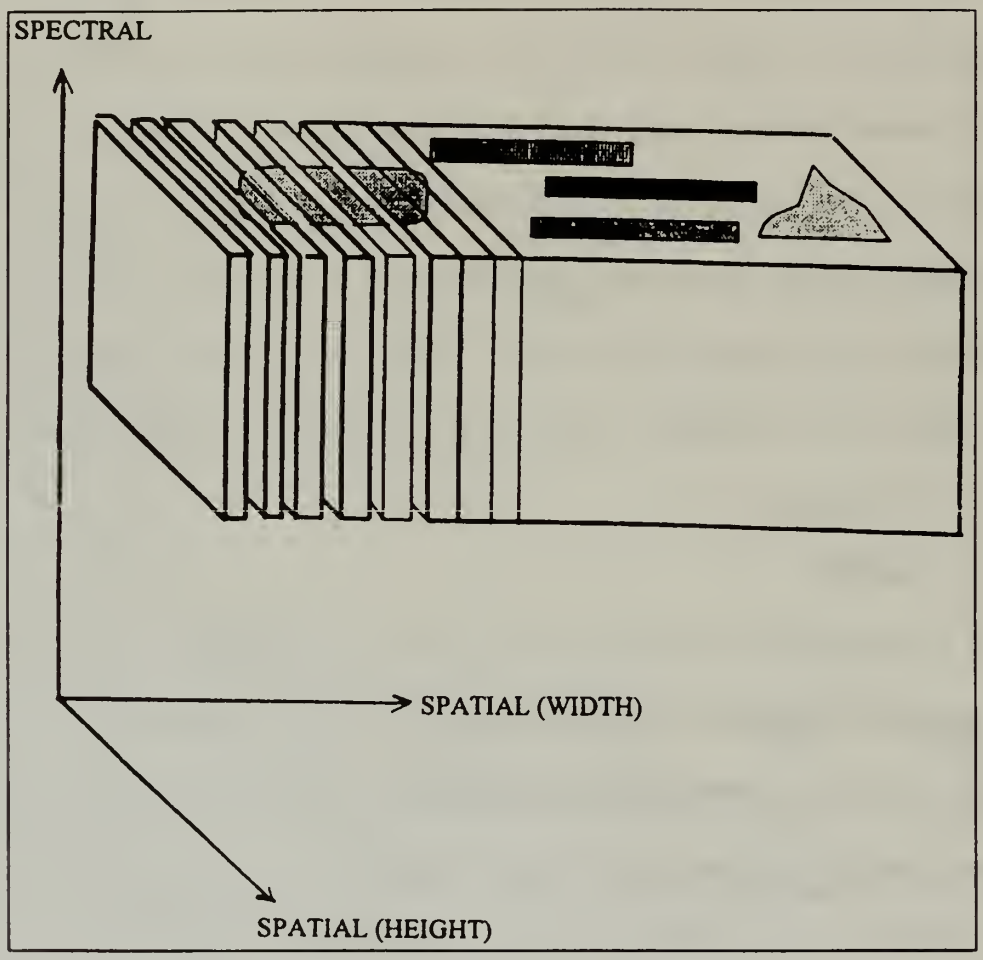


Figure 5: An image cube. From Johnson (1996).

B. SPECTRAL RESOLUTION AND REMOTE SENSING CLASSIFICATION

The spectral resolution of a sensor describes the ability to detect and record intensity differences in electromagnetic energy as a function of wavelength. The resolution needed is dependent on the materials that you want to discriminate from a scene and the confidence level desired of the discriminatory analysis. Low resolution sensors collect electromagnetic energy intensity readings across one or very few, wide

bands of wavelengths. These sensors detect general material characteristics within these wide bands. High resolution sensors collect intensity data over very small bands. Most discriminating features occur within a very small band. Remote sensors are classified by the width of the spectral bands recorded. The three classifications are multispectral, hyperspectral and ultraspectral. You can see differences in Figure 6.

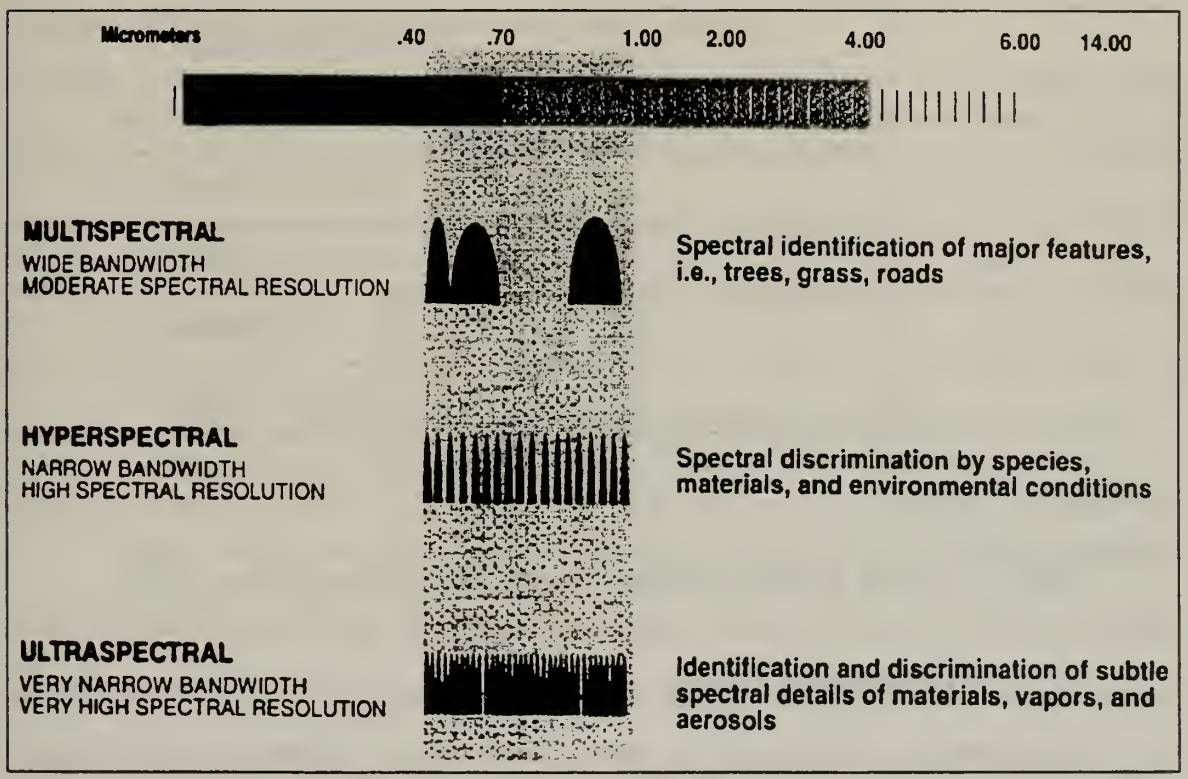


Figure 6: Classification of spectral imaging. From Multispectral Users Guide (1995).

1. Multispectral Sensors

The earliest imaging spectrometers produced were multispectral. They require less computer analysis and are easier to fabricate. These sensors look at approximately 10 bands within a spectral coverage between 400-nm and 12000-nm. The bandwidth resolution of these sensors varies. Their spectral coverage is not often continuous

throughout the entire bandwidth. Some multispectral sensors are used for terrain classification, camouflage detection, soil analysis and trafficability analysis. One well-known sensor is LANDSAT. An example of LANDSAT's multispectral characteristics is seen in Table 1.

Band Number	Spectral Bands (μm)
1	0.45 - 0.52 (blue)
2	0.52 - 0.60 (green)
3	0.63 - 0.69 (red)
4	0.76 - 0.90 (NIR)
5	1.55 - 1.75 (SWIR)
6	2.08 - 2.35 (SWIR)
7	10.4 - 12.5 (LWIR)

Table 1. Landsat Thematic Mapper Spectral Bands. From Collins. (1996).

2. Hyperspectral Sensors

Hyperspectral sensors collect scenes from tens to hundreds of bands with relatively small bandwidth resolution when compared to multispectral sensors. Development of these sensors has been relatively new as most have been built within the last fifteen years. Development has progressed due to two key component technologies. First, sensors now have better resolution. This is the ability to spectrally divide a band of wavelengths into small distinct bands. Second, detector array technology that collects the information has improved. New multi-dimensional array technology decreases the timeliness of recording and increases the resolution of the information.

Hyperspectral sensors use many techniques to select the spectrum desired including wavelength separation gratings (AVIRIS, AISA, CASI, DAIS, MOS), prisms (SEBASS,HYDICE,HRIS), fourier transform interferometers (SMIFTS,DASI) and liquid crystal tunable filters (LCTF). Some basic characteristics of three of these sensors are listed in Table 2. There are advantages and disadvantages to each technique used. Which technique you pick depends on the function of the sensor.

Instrument	Spectral Range (μm)	Number of Spectral Bands
AVIRIS	0.4 - 2.5	224
HYDICE	0.4 - 2.5	206
SEBASS	7.8 - 13.4	128

Table 2. Spectral Band Characteristics of several Hyperspectral Sensors. From Collins (1996).

Civilian and military applications for these sensors are growing as research uncovers more possible uses. Hyperspectral sensors are used for plant studies on species identification, stress, productivity, leaf water content and canopy chemistry. Soil science studies are growing with interest in type mapping and erosion studies. Geology has a large interest in mineral identification and mapping. Military uses now under investigation include target identification and classification, bomb damage assessment, terrain/ area utilization and rocket plume identification.

3. Ultraspectral Sensors

Ultraspectral classification is still under development. It will include the ability to look at thousands of bands with very small bandwidth resolution. Expected uses include

extremely specific material identification/classification and identification of aerosol and plume components of rockets and projectiles.

IV. NAVAL POSTGRADUATE SCHOOL'S ULTRAVIOLET IMAGING SPECTROMETER (NUVIS)

NUVIS is the Naval Postgraduate School's ultraviolet imaging spectrometer. It has evolved from MUSTANG (Middle Ultraviolet SpecTrograph for Analysis of Nitrogen Gases). MUSTANG was built to analyze the earth's ionosphere. A more complete description can be found in a thesis by Walden (1991). MUSTANG was involved in a project to develop an imaging spectrometer. After renaming the instrument Dual Use Ultraviolet Imaging Spectrometer (DUUVIS), Johnson (1996) designed, developed and tested it as a hyperspectral imaging sensor. His work focused on the selection and replacement of a diffraction grating and the addition of a new detector, scanning mirror and software package.

Success of Erik's work was determined by production of an image cube with two spatial and one spectral dimension. The quality and resolution were not known until completion of the design. After review of the quality, it was determined that additional changes must be made to use DUUVIS for the research we were about to embark upon. Two options to Johnson's DUUVIS were considered. The first option was to modify DUUVIS. The second option was to design and build a new instrument. The decision to build a new sensor was agreed upon after reviewing the time, money and quality considerations of both options.

This new instrument named the Naval Postgraduate School's Ultraviolet Imaging Spectrometer (NUVIS) will initially be designed to observe information in the ultraviolet portion of the spectrum. This focus is sponsored by the HYMSMO program office who is funding this instrument through the Central MASINT Office (CMO). There is interest

in finding out if any value can be attained in this portion of the spectrum. There has been no known previous hyperspectral work done on this part of the spectrum. To understand the design of this instrument, this chapter has been broken down into four sections: Telescope Assembly, Entrance Slit, Reflection Grating and Camera Assembly. Figure 7 is a sketch of this instrument.

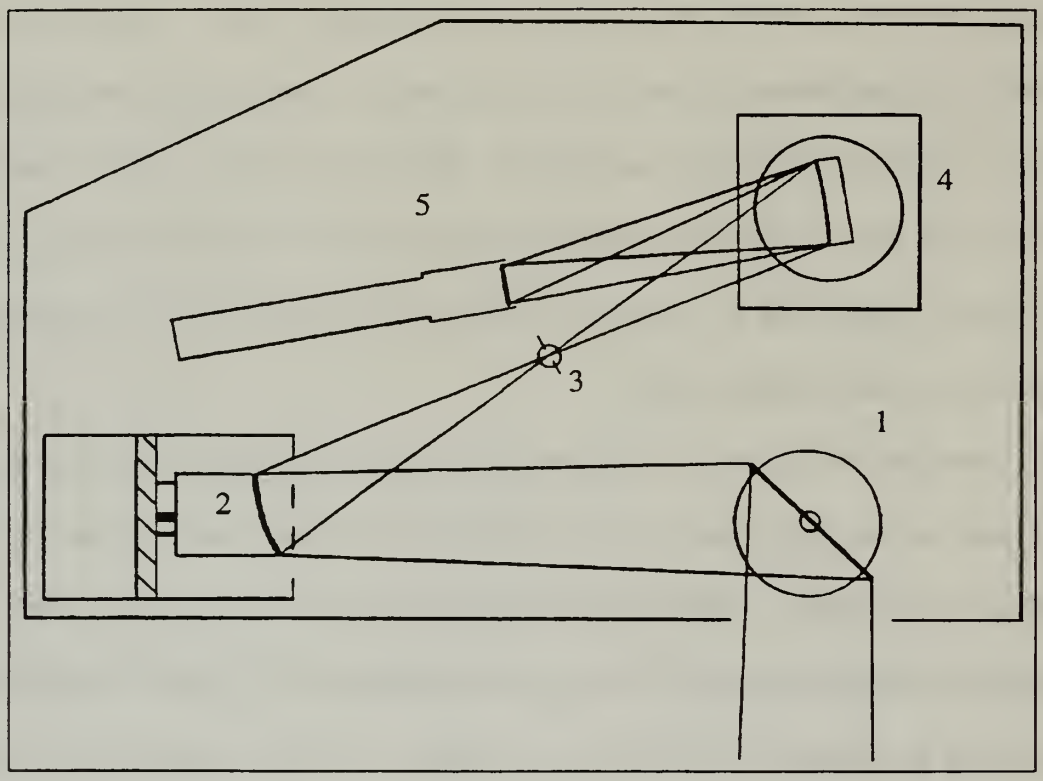


Figure 7: The Naval Postgraduate School's Ultraviolet Imaging Spectrometer (NUVIS); (1) scanning mirror assembly, (2) telescope mirror, (3) entrance slit, (4) reflection grating, (5) camera assembly.

A. TELESCOPE ASSEMBLY

The telescope assembly consists of a filter window, a scanning mirror assembly, the telescope housing, and a telescope mirror. The objective of the telescope design is focus light onto the slit. This design was built around a two inch diameter off-axis

parabolic mirror which we had on hand. Dimensions of the other components in the telescope assembly were determined by the rectangular cone of light generated by the entrance slit and the parabolic mirror.

This cone of light extending from the entrance slit past the parabolic mirror defines the light entering the sensor. Observing the light starting as a point focus anywhere within the 15 mm by 90 μm slit and ray tracing the light back past the parabolic mirror we will form a two inch collimated cone of light for each point within the entrance slit. From a point at the center of the slit, the cone formed defines the primary optical axis. The sum of all of the collimated cones defines a rectangular cone of light with rounded corners. If you were to use a ray tracing diagram to observe this cone, you would notice that the cone grows with distance from the parabolic mirror you go. The growth of the rectangular cone corresponds to a horizontal and vertical angle. These angles are called the horizontal and vertical instantaneous field of view (IFOV). At any distance from the parabolic mirror, the IFOV defines the absolute minimum size of any optical aperture used. Hooks (1997) has mathematically formulated this cone.

1. Filter Window

The filter window is a piece of color filtered glass made by Schott glass technologies Incorperated. The glass covers an opening with height and width dimensions 93 mm by 73 mm respectively. It is for the protection of the optical instrumentation inside by sealing off the sensor to everything but light. It also provides protection from physical damage caused in transportation or rough handling. This glass also filters out visible and infrared light. For more details see Hooks (1997). The size is derived from the cone of light reflected from the scanning mirror and out the

entranceway. One millimeter is added to each dimension because we did not want this opening to serve as the aperture stop to the instrument.

2. Scanning Mirror Assembly

The scanning mirror consists of a flat mirror mounted on a stepping motor. The motor is used to mechanically rotate the mirror at distinct times and angles to produce complimentary images. This complimentary image corresponds to the next slice in the formation of the image cube. Recall that to build an image cube requires a number of vertical slices of a scene. After one image or slice has been formed and recorded, the computer turns the mirror a set angle to take an image physically adjacent to the one just taken for continuous spatial information. The range of motion of the mirror defines the second spatial dimensions of the image cube not associated with the image. We have limited the range to plus or minus 10 degrees from the IFOV. The motor is adjustable if continuous spatial information is not necessary.

The mirror is made of Zerodeur coated with aluminum for reflection and sodium dioxide to protect the aluminum. Zerodeur is a strong material with a low thermal expansion coefficient. This allows for a flatter mirror. The flatness is $1/20\lambda$ at 488-nm. This means that the horizontal surface of the mirror does not deviate from a horizontal more than 24.4-nm. The size of the mirror is irregular, but cut from a 90-mm square 12-mm thick. The 90-mm was derived from the rectangular cone of light with an added 5-mm. These 5-mm account for enough mirror to physically grab and mount the mirror and does not make this mirror the limiting factor as an aperture stop. The square was then cut down on the corners to reduce the inertia produced when rotating the mirror. Recall that the rectangular cone of light has rounded corners. The edges where also cut

down to prevent chips and breakage. The 12-mm thickness was a compromise between having low mass and high flatness.

3. Telescope Housing

The telescope housing is comprised of a tube with three baffles. This tube is the light enclosed passageway from the entranceway to the parabolic mirror. The tube has three baffles to reduce off-axis, stray light. The baffles are thin aluminum plates placed in the tube. These plates have rectangular holes cut in the center. They are painted black to minimize reflected light. The dimensions of the holes are chosen to be slightly larger than the cone of light that passes through the baffles.

4. Telescope Mirror

The light from the entranceway is focused onto the slit by an off-axis parabolic mirror. This mirror was picked for its availability, compact size and quality as a focusing mirror. It is a Space Optics Research Labs (SORL) 2 inch diameter mirror, sales order number SN4338, with an off axis distance of 2.5 inches. It is made of Zerodeur coated with $AlMgF_2$. The aluminum is to reflect the light and the MgF_2 is to protect the aluminum. The reflectance has been tested to be above 95% for wavelengths above 280-nm.

B. ENTRANCE SLIT

The entrance slit has a height and width of 15-mm by 90-μm respectively. Light from the scene is focused onto this slit. The dimensions of the slit were chosen based on a number of factors. A height of 15-mm was chosen to maximize the use of the detection surface. The detection surface is the image intensifier surface and is round with a diameter of 25-mm. A width of 90-μm is derived from the size of three pixels on the

camera. Light that hits three pixels is reduced in a fiber optic bundle from the light that hits the image intensifier. The light that hits the intensifier corresponding to three pixels is 90-μm wide. Three pixels were chosen to over sample the light. This oversampling improves the confidence in results. As stated before, the slit also defines the rectangular cone of light and IFOV. This instrument's Instantaneous Field of View (IFOV) is 5.2° in the vertical direction and 0.031° in the horizontal direction. This IFOV with the distance from a scene gives a ground target area. As an example, if this sensor is flown on an aircraft at 3,000-meters, the ground target area or footprint is 273-m by 1.6-m. This footprint is one slice of the image cube.

The mechanical drawing in Figure 8 shows that the slit is built into a cylindrical base. The cylindrical base makes it easy to move the slit around when trying to get the proper placement. The opening in the base holds a rectangular piece of aluminum with the slit centered as seen in Figure 9. This allows for easy replacement of slits of different sizes. The slit was constructed by gluing two razor blades onto the piece of aluminum. The details of the construction and placement of the slit are discussed in the next chapter.

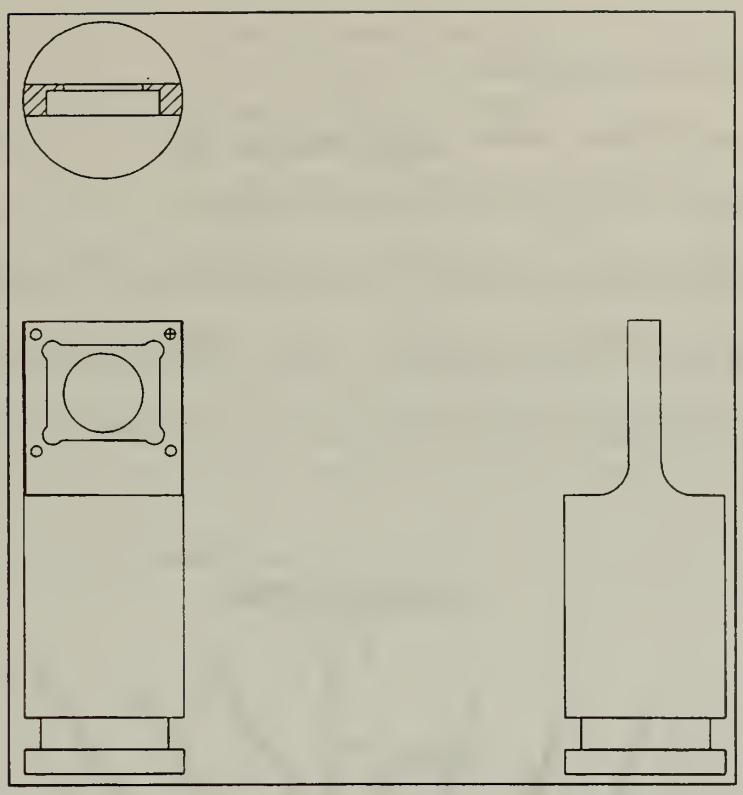


Figure 8: The entrance slit holder.

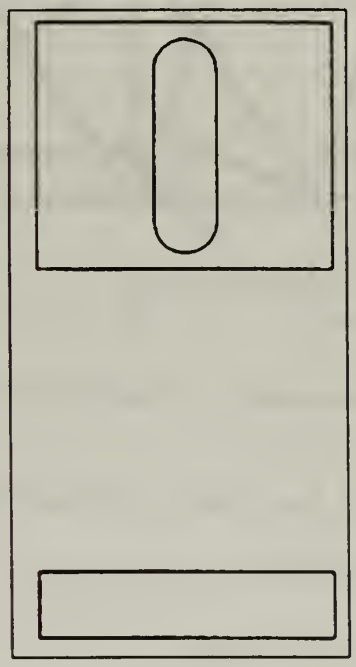


Figure 9: The entrance slit before razor blades are attached.

C. REFLECTION GRATING

The grating diffracts incident light from the slit in the horizontal dimension forming a spectrum. The amount of horizontal separation for two given wavelengths depends on the incident angle of incoming light and the spacing of grooves constructed on the grating. Where you place the detector relative to the grating defines the separation and bandwidth of the light recorded. Diffraction can be visualized by the geometry in Figure 10.

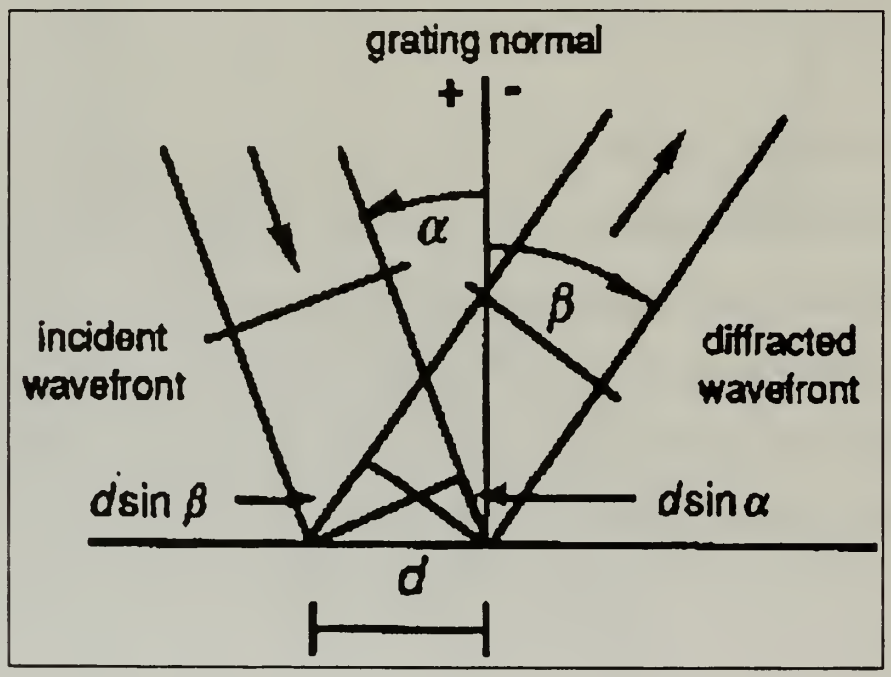


Figure 10: Diffraction geometry. From Milton Ray Company (1994).

Equation 1 describes the figure and is referred to as the grating equation. This equation holds for the grating in NUVIS to the first order.

$$n\lambda = d \sin\alpha - d \sin\beta \quad (1)$$

Where:

n = order of spectral interest
λ = wavelength of interest
α = angle of incident of light
β = diffraction angle
d = separation distance of the grooves

The grating used in NUVIS is a Instruments S.A. (ISA) flat field, imaging, aberration-corrected, holographic concave grating. It's diameter is 50-mm with 1200 grooves per mm and an F/# of 3.2. For best results, ISA recommends the geometry according to Figure 11. This optical diagram results in a 25-mm detector recording wavelengths between 300- and 400-nm.

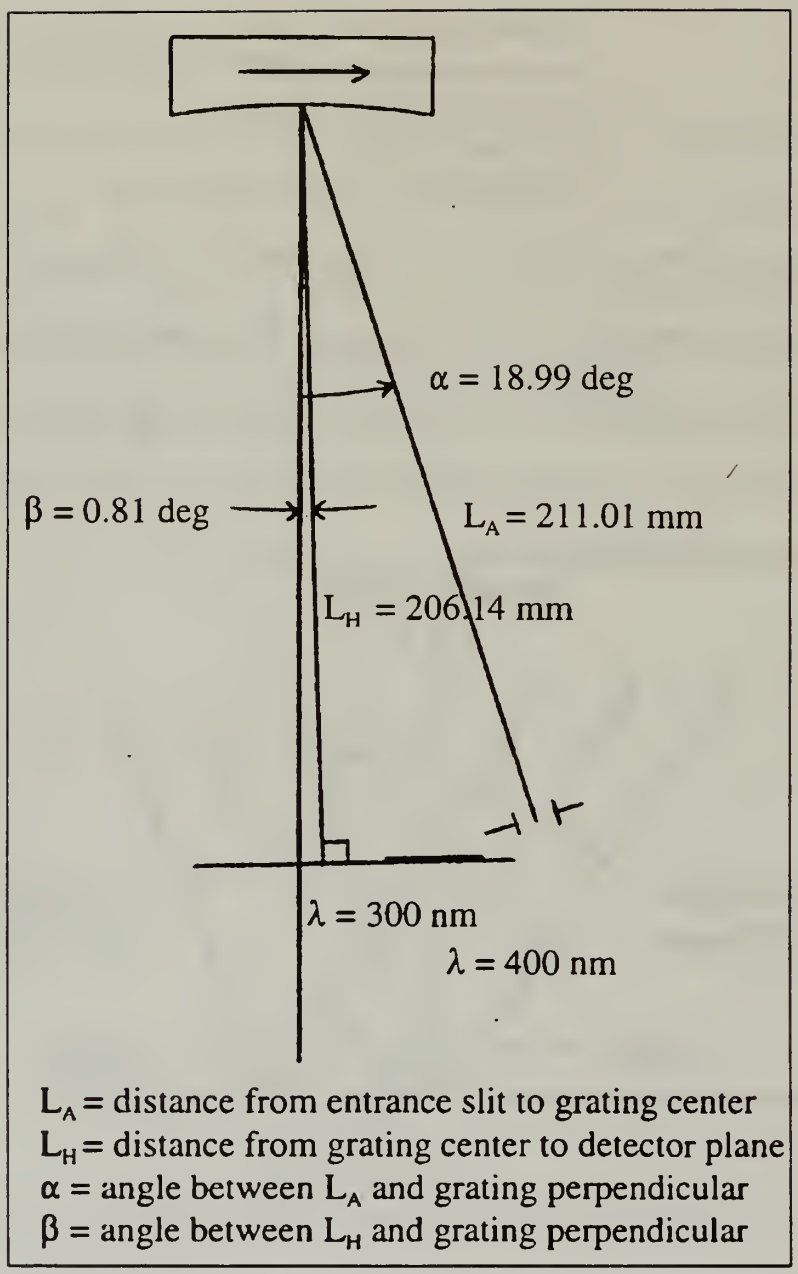


Figure 11: Geometry of the entrance slit and the detector relative to the grating recommended by Instruments S.A., Inc. After Jiang (1997).

D. CAMERA ASSEMBLY

The function of the camera assembly is to record the light reflected from the grating. It records intensities of light separated by wavelength in the horizontal direction,

while keeping the spatial integrity of the scene in the vertical direction in tact. The camera assembly includes an image intensifier optically coupled to a charge coupled device (CCD) camera by a fiber optic bundle. The CCD camera output is sent directly to a Sony compact computer.

1. Image Intensifier

The image intensifier is a proximity focused channel intensifier tube with dual microchannel plates. This image intensifier serves two purposes. First, this intensifier increases the intensity of the light for more pronounced images on the detector. The intensity must be increased because, as seen in the discussions of light in the atmosphere, solar illumination is low in the ultraviolet portion of the spectrum. Second, the intensifier will produce photons of a different wavelength from the photons entering the intensifier in order to match the camera's peak sensitivity (Figure 12). The peak sensitivity is in the visible spectrum between 500- to 650-nm. The image intensifier will produce light between 500- and 630-nm. The image intensifier retains positional information and relative intensity therefor our spectral and spatial input is related to the output.

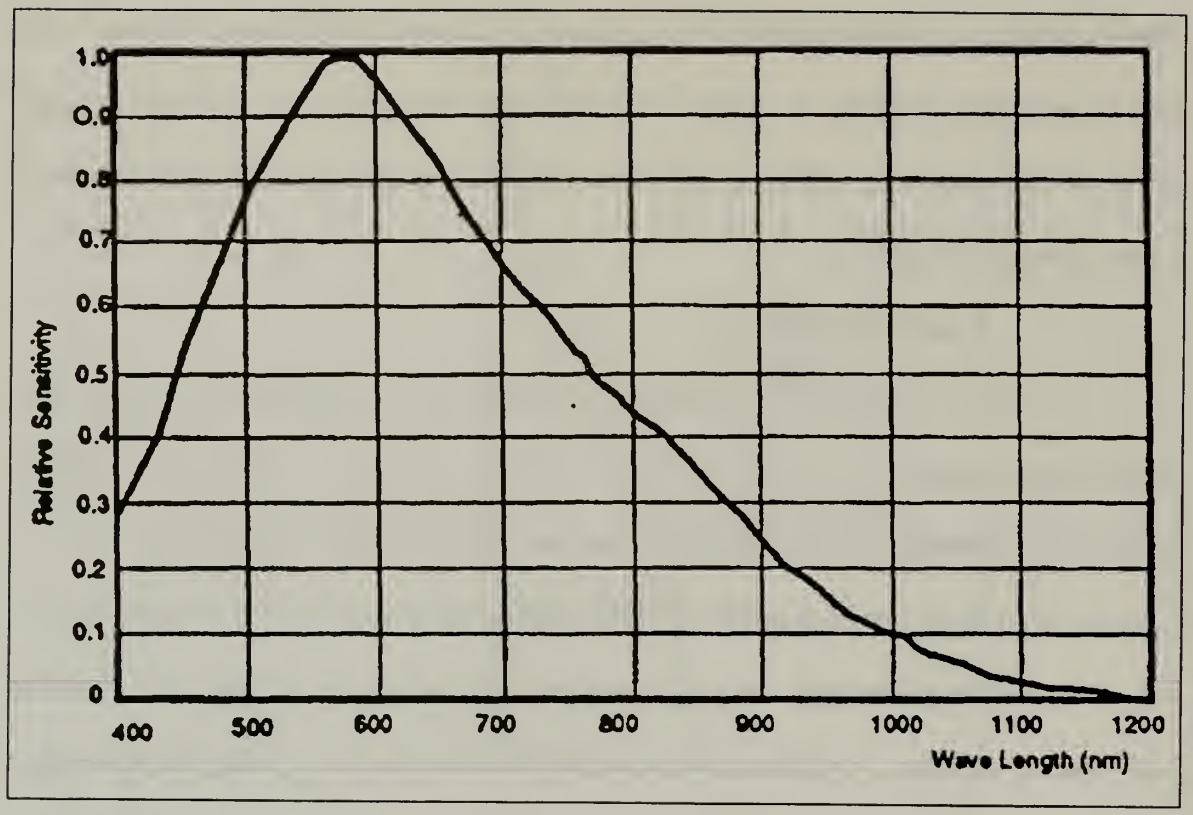


Figure 12: The sensitivity of the Pulnix TM-745 high resolution camera. From Pulnix.

The image intensifier consists of a quartz window, a photocathode, two microchannel plates, a phosphor screen and a fiber optic faceplate on the back-end to transport the output light to the detector.

a. Window

This window protects the intensifier. It is made of suprasil. This window material was used because of its high transmittal down to 200-nm. The first thing light encounters past the window is the S-20 photocathode.

b. S-20 Photocathode

A photocathode is designed to turn photons into electrons. The S-20 refers to the semiconductor material in the photocathode. This photocathode is sensitive

to light between 200- and 520-nm (Figure 13). Photocathodes work on a principle known as the photoelectric effect.

Photoelectric effect is the physical process where a photon strikes a material and ejects an electron from this material. The quantum efficiency, seen in Figure 13, is in the range of 10 - 30 %.

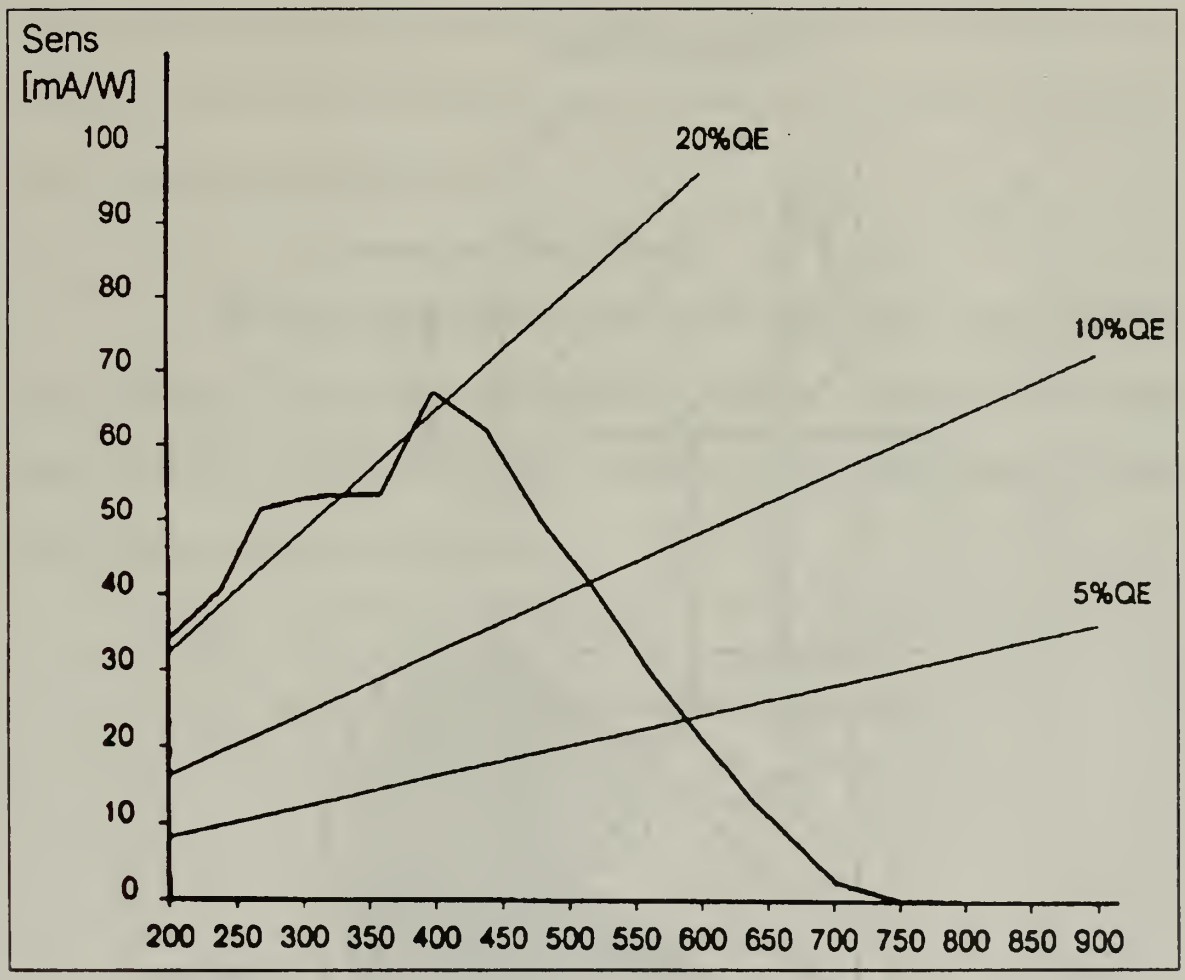


Figure 13: Photocathode sensitivity and quantum efficiency. From DeBarry (1997).

Figure 14 shows the energy band diagram of a semiconductor showing the photoelectric effect. As a photon strikes the material, the material absorbs its energy (E). This energy excites an electron to a new energy level. This energy level must be higher than

conduction band energy (E_c) plus the electron affinity (χ). This excited electron will diffuse through the material and then escape. During this diffusion the electron will lose some thermal (kT) energy to the lattice, but not enough to hinder the escape. As long as the material is not in equilibrium, this electron, sometimes called a "hot" electron, has a high probability of escape.

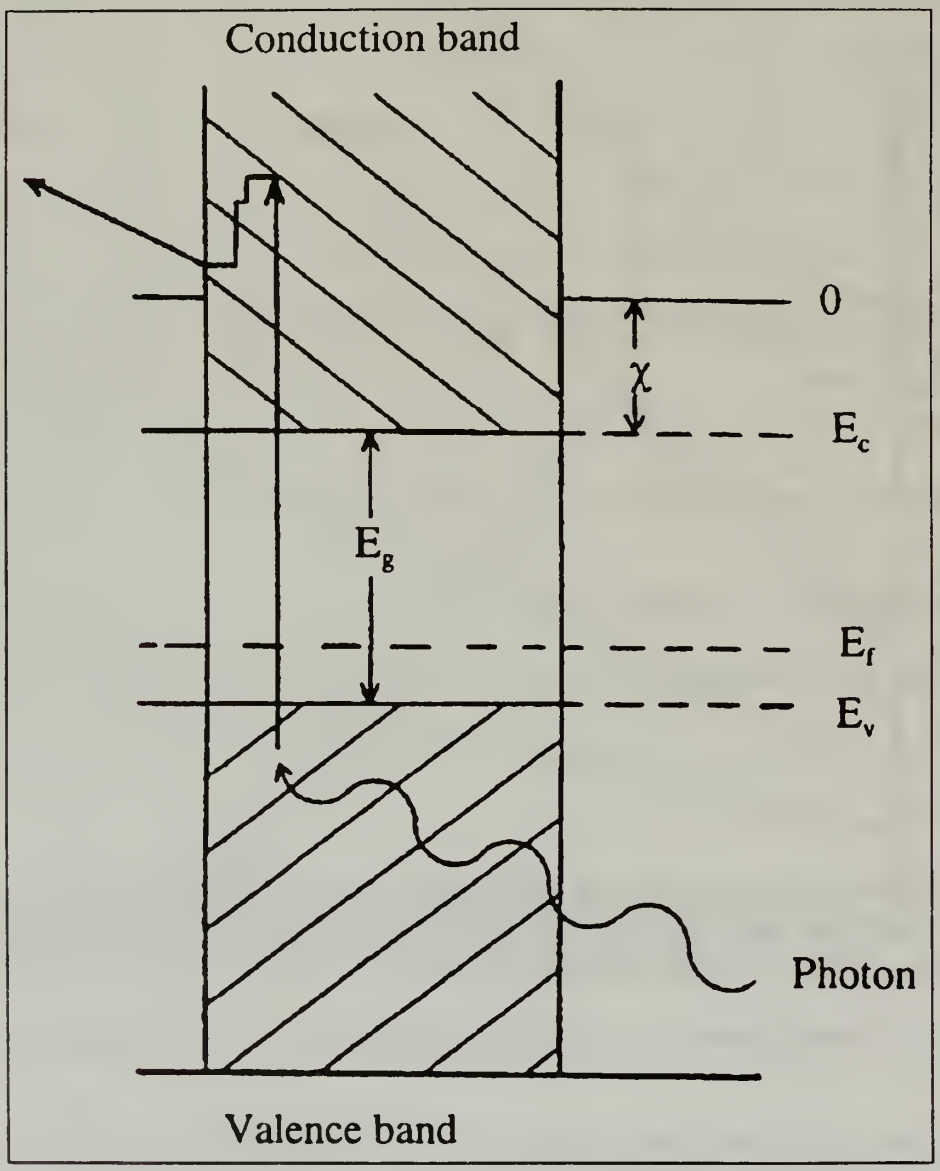


Figure 14: Photoelectric effect in a semiconductor. After Reike (1994).

The thickness of the semiconductor needs to be thick enough for absorption of the photon, but thin enough for the diffusion of the electron. The thickness is usually on the order of just less than the diffusion length for electrons and will coincide with the absorption length of the photons. Absorption length is dependent on wavelength and material and therefore can be calculated. The doping of a material is critical to arrive at a desired thickness. The photocathode's efficiency is dependent on the transmittance of the surface and the probability of electron escape by diffusion. The escaping electrons are then directed to the microchannel plate.

c. Microchannel Plate Assembly

The microchannel plate assembly (MCP) is comprised of about 5 million glass capillaries or channels within a casing with 1,600 volts DC across that casing. Figure 15 shows a cross-section of a MCP. The inner diameter of each channel is 10-μm with a center to center distance of 12-μm.

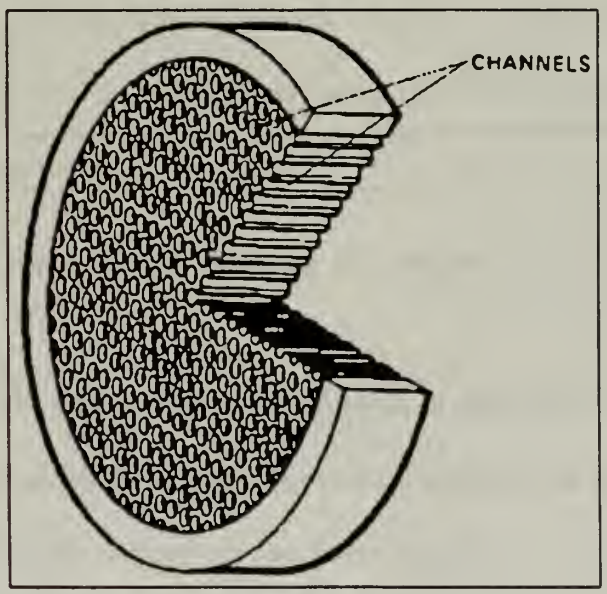


Figure 15: MCP construction. From Hamamatsu Photonics (1985).

Each capillary or tube acts as a multiplier. As an electron enters a tube, it collides with the walls of the tube causing secondary electrons to be stripped from the walls. The voltage applied across the tube acts as an electron accelerator. These secondary electrons also collide with the wall before exiting and in turn knock off more electrons eventually causing a large number of electrons to exit the tube. The cascading of electrons results in about 100,000 electrons exiting for every one that enters. This cascading is seen in Figure 16.

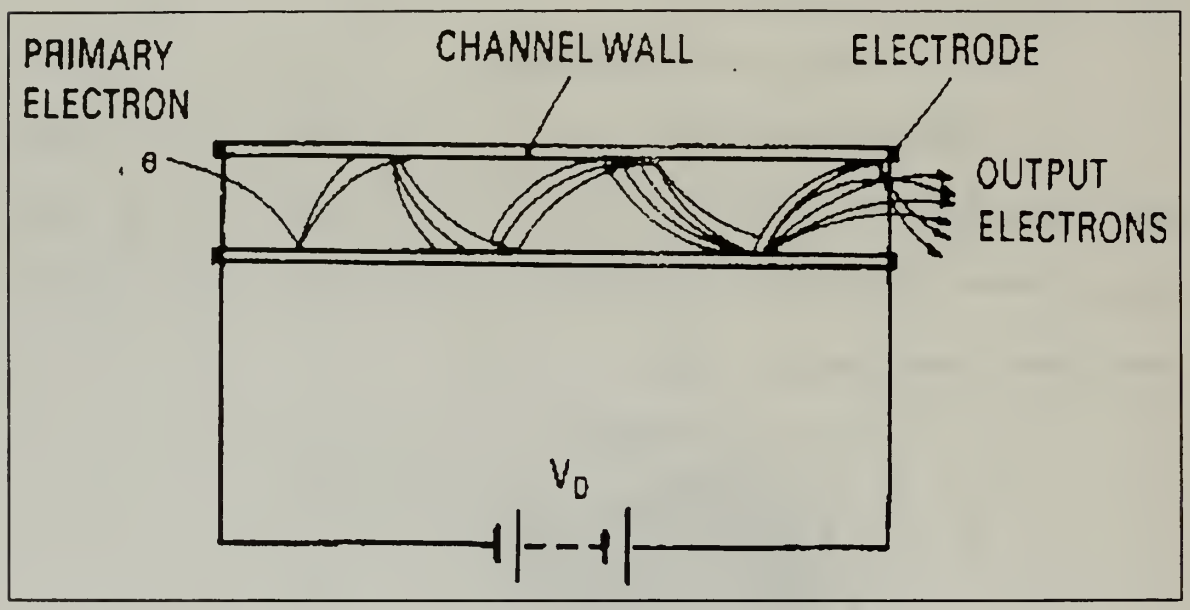


Figure 16: Electric representation of electron amplification. From Hamamatsu Photonics.

The microchannel is made of a lead-oxide glass. The inner surface of the tube is hydrogen fired on assembly leading to a breakdown of the glass and formation of a lead-oxide (PbO) layer. Electrons break off the surface when hit by other electrons with large velocities. The surface will conduct current to replace lost charge due to the cascading of electrons from the tube. These tubes do have current limitations. If the

limitations are exceeded, you have dark currents reducing the signal-to-noise ratio. Dark current here refers to thermionic emission. Typically dark currents in these channels run around 10 counts per second per centimeter squared. The dark current will be measured during calibration and is typically low for these types of detectors. The amplified electron beam exiting the MCP is accelerated by voltage onto a phosphor screen.

d. P-20AF Phosphor Screen

The P-20AF screen refers to a photon-producing screen made of aluminum with a phosphor coating. The aluminum is on the photocathode side of the screen to prevent transmission of photons returning into the system and corrupting its efficiency. The phosphor releases energy in the form of light. This process is almost the opposite as when we turned the photons into electrons. Figure 17 shows an example of how a phosphor works. The phosphor is made up of a material that has p-type and n-type impurities imbedded. In equilibrium both impurities are charged. An electron coming from the MCP frees electrons and holes in the material. Both charge carriers wander until they are captured by a charged impurity atom that emits a photon when the system attempts to return to the equilibrium state.

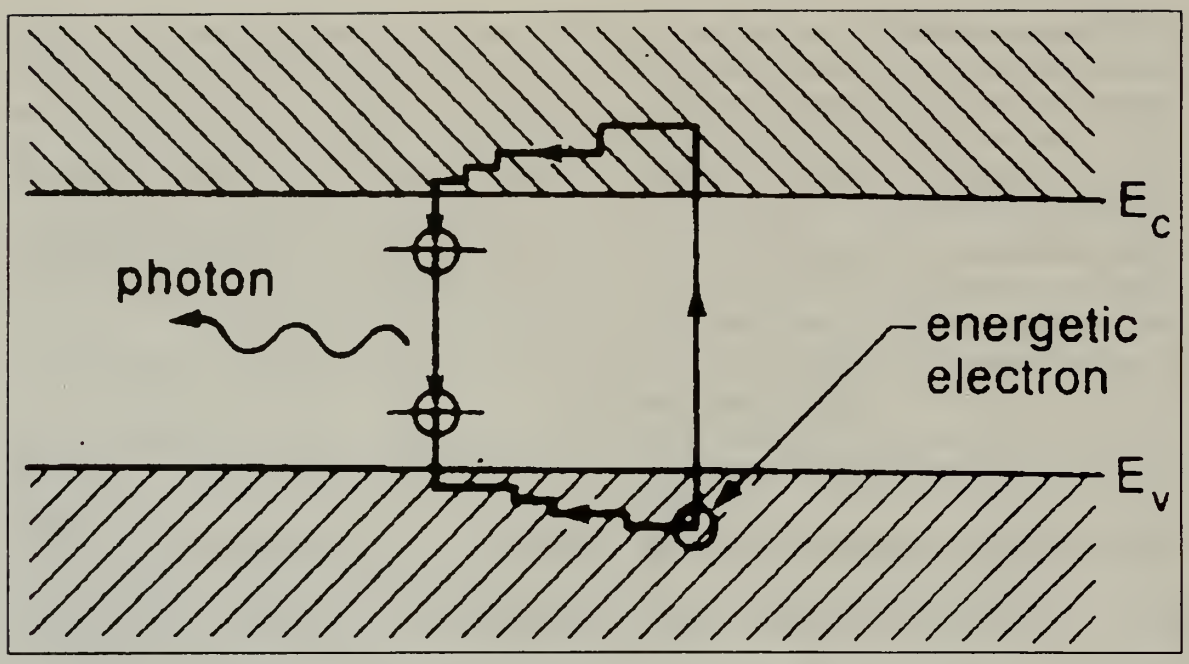


Figure 17: Process of luminescence of a phosphor. From Reike (1994).

The phosphor of the proximity-focused image intensifier is in close proximity to the photocathode. This proximity reduces spreading to retain resolution. The light that is emitted from this intensifier has a wavelength range of 500 – 630-nm. These wavelengths are a function of the phosphor. Light exits the intensifier with irradiance information through a fiber optic bundle to be recorded by the detector for transfer into data.

2. Charge Coupled Device

Both the exit windows of the intensifier and the entrance to the detector are fiber optically connected for minimal loss of information. The fiber is tapered to take the information from the 25-mm intensifier and transfer it to a 2/3-inch photon detector. The detector accepts light from the intensifier, changes it into an analog signal to record the

irradiance within each pixel and then transfers into digital form before storing in the computer.

The photon detector is called a Charge Coupled Device (CCD). This device is segmented into 768 (horizontal) by 494 (vertical) pixels with a cell size of 11(H) x 13(V)-μm. Referring to Figure 18(a), each pixel contains a metal-oxide-semiconductor (MOS) grown onto a single piece of silicon. A metal electrode has also been evaporated onto this oxide layer which insulates against the passage of electrons from the silicon onto the electrode. The silicon is doped p-type. When a positive voltage (V_g) is placed on the electrode, the holes in the p-type silicon will tend to drift away from the electrode causing a depletion region in the vicinity of the electrode. The voltage is providing bias on the device. This bias changes the energy levels in the material and a potential energy well forms (Figure 18 (b)). Now, if any free charge carriers accumulate in the silicon they will be trapped between the silicon and the oxide layer (Figure 18 (c)). The incoming photons are absorbed by the silicon which will produce a current that flows between the contacts. The thickness of the region will dictate the sensitivity of the device.

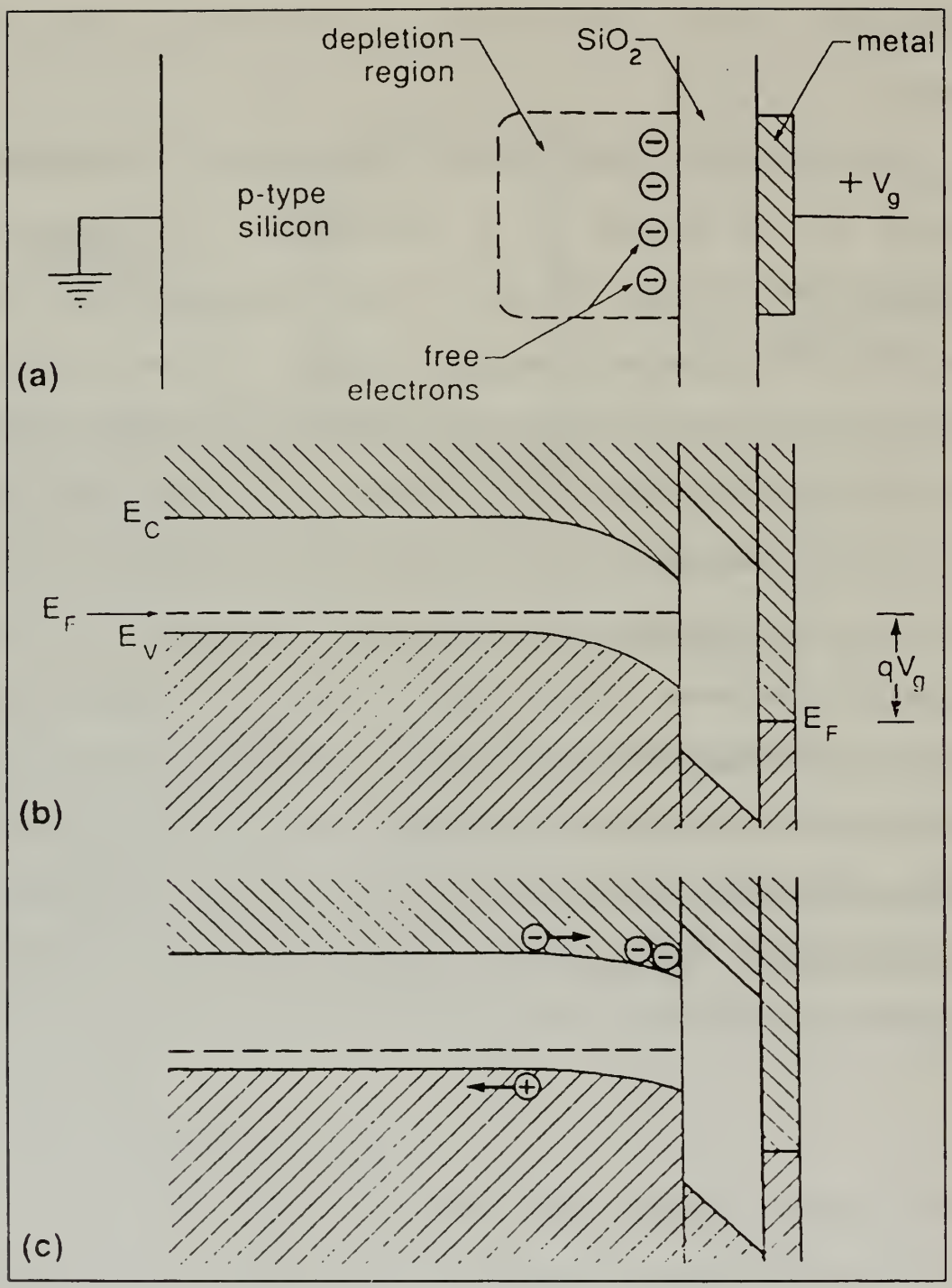


Figure 18: Charge collection at a single pixel of a CCD: (a) illustrates the collection of free charge carriers at the S1O2 interface, (b) shows formation of a potential well after a voltage is applied, (c) shows collection of charge carriers in the potential well. From Reike (1994).

There are three functions to the operation of the CCD. The first two functions are related. They are conversion of the photons to electrons and collection of these electrons. Photons enter the MOS and create free electrons in the depletion region or diffuse into the depletion region and collect at the boundary. This process reduces the quantum efficiency. Diffusion of electrons is not 100% effective and not all of the electrons will reach the depletion region. The number of electrons that do accumulate is directly proportional to the same number of photons that have been absorbed into the silicon. There is a small possibility of thermal excitation creating electrons in the device. With the wavelengths we are working with this is not expected to cause problems at room temperatures. Calibration of NUVIS will determine the effect of thermal excitation. At some time after the device has accepted photons there will be a finite number of electrons collected in each potential well.

The third function of operation is transmission of charge. During this function, there are no more incoming photons and the potential well of each MOS has accumulated electrons. Each well is part of a two dimensional array which makes up the CCD. The CCD has the ability to change the voltage of each well. Changing the voltage will raise or lower the level of the potential well. This property is used to transfer charge. When the voltage is decreased, the lowering of the well transfers charge into the adjacent well. Horizontal or vertical transfer is accomplished by varying voltages applied to the adjacent horizontal and vertical wells. All of the accumulated electrons will eventually end up in the corner well. This last well will empty via an analog signal through the electrode. The entire array will empty prior to another image being collected.

This analog signal is then transferred to an analog-to-digital converter and then saved by a computer in a TIFF file. This leads to many files with irradiance information of each pixel of each image. Together these files produce a hyperspectral cube from an area of interest. This accumulation of massive amounts of data is a leading cause for the slow development of algorithms and analysis techniques that produces useful information. The leading edge of remote sensing involves taking these large amounts of data and figuring out what is a relevant and developing techniques for quickly reducing the irrelevant to exploit the useful data.

V. ALIGNMENT, PLACEMENT AND CONSTRUCTION

After a detailed explanation of the individual parts of NUVIS, this section is a collection of remaining details that make NUVIS a viable remote sensor. The alignment of the parabolic mirror and the placement of the entrance slit are dependent functions and must be addressed together. Similarly, the placement of the reflection grating and camera assembly is accomplished by an iterative, co-dependent process and must be explained together. Lastly, a description of how the entrance slit was assembled and aligned with the base will be explained.

A. TELESCOPE MIRROR ALIGNMENT AND ENTRANCE SLIT PLACEMENT

The individual parts of the sensor are secured on one piece of aluminumthat was weight-relieved in a honeycomb pattern. To ensure that the optical placement remained accurate when the optics were transfered from the table to the aluminum plate, all measurements were taken relative to some base piece. The base piece used for this purpose was the base of the telescope mirror. This base piece was alligned to the corner of the bench. The optical axis of the off-axis parabolic mirror was defined to be parallel to one edge of the table. It is important to note here that there are many rows of holes in the optical bench and these holes are also parallel to the edge of the bench. To get the optical axis parallel to the bench takes several steps and the process includes placement of the entrance slit at the same time.

First, a helium-neon laser was secured to one end of the optical bench and its beam was alligned parallel to the surface of the optical bench.. A height guage was used to accomplish this. The laser beam was also alligned parallel to the edge of the bench.

Again the height guage was used to ensure that the beam was alligned with a row of holes in the bench.

The next step was to secure the telescope mirror assembly along this same row of holes at the opposite end of the bench from the laser. The telescope mirror assembly includes an alignment mirror mounted on top of the parabolic mirror. This alignment mirror was pre-adjusted by SORL to have an optical axis parallel to that of the parabolic mirror. The laser beam was adjusted vertically until the beam was the same height off the bench as the alignment mirror while maintaining the overall alignment with the table. The telescope mirror assembly was then adjusted until the laser reflected from the alignment mirror back onto the exit aperture of the laser. The parabolic mirror was considered aligned with the edge of the bench and parallel with the surface. The alignment mirror was then taken off of the telescope assembly.

To complete the alignment of the parabolic mirror, it was rotated about the optical axis until the focus point was at the same height as the slit. To adjust the rotation, a pinhole and an alignment telescope was needed. For a pinhole we replaced the entrance slit in the slit holder with a pinhole. This pinhole position corresponds to the center of the entrance slit. An alignment telescope focused at infinity was placed approximately on the optical axis where the laser was located. Using a lamp, the backside of the pinhole was illuminated. Looking through the alignment telescope, we move the slit holder until the pinhole was focused. Then we secured the holder to the bench at this position. Using the rotation adjustment knob on the telescope mirror, we rotate the mirror until the best focus of the pinhole was seen through the alignment telescope. The parabolic mirror was then aligned and the slit holder positioned to place the slit at the focus point of the mirror.

B. REFLECTION GRATING AND CAMERA ASSEMBLY PLACEMENT

Due to difficulty in obtaining the detector, the alignment of the grating and the camera assembly was left to others. This section describes what should be done for this alignment. The placement of the reflection grating and camera assembly is accomplished through an iterative process. Figure 11 is the ISA recommended placement of the grating relative to the entrance slit. Physical placement can only be accomplished by eyeball approximation and is not guaranteed to be the exact placement to produce the best results. The process we will use starts with this approximate placement. The entire sensor must also be used. A mercury lamp with known ultraviolet spectral lines is placed several meters from the sensor. Observed spectral spots on the computer screen are examined. Then the grating will be moved and the spots re-examined for the best focus. Once this focus is determined, the camera assembly will be moved to another position. The grating is then adjusted again until this best focus is found. The two best focus spots are compared. This process is repeated until the overall best focus is found for placement of both the grating and camera assembly. These positions are then secured to the bench. Once all positions are secured on the bench, measurements are taken in order to repeat these placements on the baseplate.

C. ENTRANCE SLIT CONSTRUCTION

The entrance slit was constructed using an alignment tool to glue two razor blades to a rectangular piece of aluminum. The aluminum piece fits into the slit holder. Figures 10 and 11 show mechanical drawings of the slit holder and the aluminum, rectangular insert. The insert has an oval hole cut in the middle. The long axis of the oval is vertical and 15 mm at its maximum. An alignment tool, seen in Figure 19, was fabricated to align

a vertical edge of the tool 45-μm from the center of the oval. It also ensures that this edge is parallel to the side of the aluminum rectangle and therefor is perpendicular to the base of the slit holder. One razor blade is the placed touching this alignment tool while the glue hardens. After the first blade is secure, a 90-μm gauge is placed against this blade. The second blade is then glued next to the gauge ensuring a 90-μm by 15-mm entrance slit.

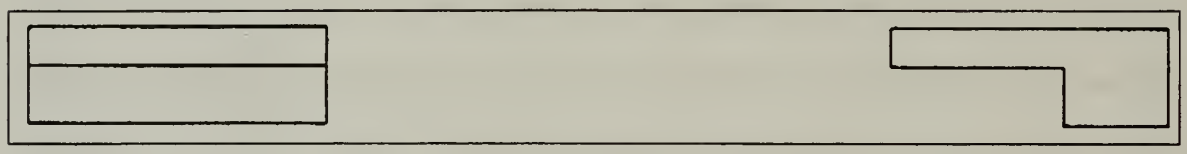


Figure 19: The alignment tool used to place razor blade on entrance slit.

VI. SUMMARY AND RECOMMENDATIONS

Originally, the intent of my thesis was to produce ultraviolet data from a scene using a remote sensor. DUUVIS, the intended sensor, proved to be inadequate to produce useful results. My thesis evolved into designing and building a new hyperspectral remote sensor: NUVIS. This thesis is a complete description of the parts used to build NUVIS and some of the techniques to geometrically place the parts. At the time of writing, this instrument is still not complete. The fiber bundle fusing of the image intensifier to the camera has been delayed several months by the contractor. Until this assembly is returned, placement of the grating and camera assembly cannot be completed. Until each piece is properly placed, calibration and testing cannot take place.

When the camera assembly is returned placement of the grating and camera assembly must be accomplished before the instrument is operational and testing begins. The placement technique has already been addressed. The first test of NUVIS will be accomplished while the placement of the grating and camera assembly is completed. During the placement process, the spectra of a mercury lamp will be recorded. The spatial properties of NUVIS will not be examined during this process. A test to evaluate spatial properties will involve taking images in a darkened lab using a mercury lamp behind a cardboard shield. The shield will have a design cut through the cardboard that has spatial dimensions. With the shield placed within the ground target area of one image, the image will be recorded and observed for spatial resolution. After this test, NUVIS will be ready for final assembly and testing outside the lab.

Outside testing plans first include a roof test. The roof test takes place on the roof of a six story building on the campus of the Naval Postgraduate School. After placing NUVIS on a secure telescope tripod, the ground target area will be calculated and identified for one image and a full scan. First, the lamp with shield will be placed within the one image ground target area. During this experiment the lab experiment will be reproduced from the roof. The subsequent recorded image will be compared to the lab image. Second, the lamp with shield will then be placed within a full scan of NUVIS and the images recorded. Lastly, military camouflage netting and pieces of metal with military paint will be placed within the full scan. The lamp and shield will remain within the scan. This last set of images will be compared to the first scan to determine if any value can be recognized from the images concerning military objects.

Future tests beyond The Naval Postgraduate School include possible tower tests, aircraft tests and volcano tests. If the roof top tests show producible value, then the tower test will proceed. A tower test involves taking several scans from a tower on a hill. Several different targets of military value will be placed within the ground target area of the scan. The results will then be examined. Aircraft tests are an extension of tower tests from a different platform with a different ground target area. Volcano experiments will examine the ability of NUVIS to identify SO_2 gases. SO_2 is very common with volcanoes and is common with rocket plume exhaust gasses.

These plans are long in the future, but they show the abilities and associated value NUVIS is capable of. Each step in the future for NUVIS will take time and careful examination. With luck, knowledge, and patience NUVIS will evolve into an important sensor capable of providing important military value.

LIST OF REFERENCES

Atkinson, J. D. IV, "Implementation and use of a computational ray-tracing program for the design and analysis of complex optical systems", Master's Thesis, Naval Postgraduate School, Monterey, California, (1993).

Collins, Brian H., "Thermal Imagery Spectral Analysis", Master's Thesis, Naval Postgraduate School, Monterey, California, (1996).

DeBarry, Keith A., Ziemer & Associates, Inc., private conversations (1997).

Elachi, Charles, *Introduction to the physics and Techniques of Remote Sensing*, John Wiley and Sons, New York, 1987.

Hamamatsu Photonics, *Characteristics and Applications of Microchannel Plates*, (1985).

Hooks, T., "The design and construction of the Naval Post Graduate School's Ultraviolet Imaging Spectrometer (NUVIS)", Master's Thesis, Naval Postgraduate School, Monterey, California, (1997).

Jiang, Wu, Instruments S. A. Inc., private conversations (1997).

Johnson E. O., "Design, development, and testing of an ultraviolet hyperspectral imager", Master's Thesis, Naval Postgraduate School, Monterey, California, (1996).

Kuo-Nan Liou, *An Introduction to Atmospheric Radiation*, Academic Press, Inc., London, 1980.

McCoy, R. P., Wolfram, K. D., Meier, R.R., Paxton L.J., Cleary, D. D., Prinz, D.K., Anderson Jr., D. E. "The Remote Atmospheric and Ionospheric Detection System". *Proceedings of SPIE*, The International Society for Optical Engineering, Vol. 687, p. 142, 1986.

Milton Roy Company, *Diffraction Grating Handbook*, 2nd ed., (1994).

Multispectral Users Guide, Department of Defense, August 1995.

Pulnix, *Operations and Maintenance Manual of the TM-745 / TM-765 High Resolution CCD Camera*, (1996).

Reike, G. H., *Detection of Light: From the Ultraviolet to the Submillimeter*, Cambridge University Press, Cambridge, 1996.

Stregis, C. G., " Atmospheric transmission in the middle ultraviolet". *Proceedings of SPIE*, The International Society for Optical Engineering, Vol. 687, P. 2, 1986.

Walden, B. S., "An analysis of middle ultraviolet dayglow spectra", Master's thesis, Naval Postgraduate School, Monterey, California, (1991).

INITIAL DISTRIBUTION LIST

No. of copies

1. Defense Technical Information Center 2
   8725 John J. Kingman Rd. STE 0944
   Ft. Belvoir, VA 22060-6218

2. Dudley Knox Library 2
   Naval Postgraduate School
   411 Dyer Rd.
   Monterey, California 93943-5000

3. Director, Training and Education 1
   MCCDC, Code C46
   1019 Elliot Road
   Quantico, VA 22134-5027

4. Director, Marine Corps Research Center 2
   MCCDC, Code C40RC
   2040 Broadway Street
   Quantico, VA 22134-5107

5. Director, Studies and Analysis Division 1
   MCCDC, Code C45
   3300 Russell Road
   Quantico, VA 22134-5130

6. Marine Corps Representative 1
   Naval Postgraduate School
   Code 037, Bldg. 234, HA-220
   699 Dyer Road
   Monterey, CA 93940

7. Marine Corps Tactical Systems Support Activity 1
   Technical Advisory Branch
   Attn: Maj J.C. Cummiskey
   Box 555171
   Camp Pendleton, CA 92055-5080

8. Dr. David D. Cleary 3
   Physics Department, PH-CL
   Naval Postgraduate School
   Monterey, California 93943-5000

9. Major Andrew R. Macmannis 3
C/O Barbara Owens
1865 Hubbard Rd.
East Aurora, New York 14052

10. Dr. William. B. Meier II, Chairman PH 1
Physics Department, PH-WB
Naval Postgraduate School
Monterey, California 93943-5000

11. Dr. R. C. Olsen 1
Physics Department, PH-OS
Naval Postgraduate School
Monterey, California 93943-5000

DUDLEY KNOX LIBRARY
NAVAL [illegible] SCHOOL
MONTEREY CA [illegible]-5101

DUDLEY KNOX LIBRARY
3 2768 00340861 8